Quantum Monte Carlo calculation of the Fermi-liquid parameters in the two-dimensional electron gas

Yongkyung Kwon
Department of Physics and Materials Research Laboratory, University of Illinois at Urbana-Champaign, Urbana, Illinois 61801

D. M. Ceperley
Department of Physics and National Center for Supercomputing Applications, University of Illinois at Urbana-Champaign, Urbana, Illinois 61801

Richard M. Martin
Department of Physics and Materials Research Laboratory, University of Illinois at Urbana-Champaign, Urbana, Illinois 61801
(Received 31 January 1994)

Excitations of the two-dimensional electron gas, including many-body effects, are calculated with a variational Monte Carlo method. Correlated sampling is introduced to calculate small energy differences between different excitations. The usual pair-product (Slater-Jastrow) trial wave function is found to lack certain correlations entirely so that backflow correlation is crucial. From the excitation energies calculated here, we determine Fermi-liquid parameters and related physical quantities such as the effective mass and the Landé g factor of the system. Our results for the effective mass are compared with previous analytic calculations.

I. INTRODUCTION

There has been a great deal of interest in the two-dimensional (2D) electron gas which can be realized at interfaces of $GaAs/Al_xGa_{1-x}As$ heterostructures and metal-oxide-semiconductor structures.[1] Since the electron density can be varied over a wide range, this system provides a useful model of many-body effects in two dimensions. Furthermore, the fractional quantum Hall effect and high-T_c superconductivity have generated more interest in this system because they are believed to be 2D phenomena occurring in a strongly-correlated electron system.

Since the experimental work of Fang and Stiles[2] on the anomalous Landé g factor g^* and of Smith and Stiles[3] on the many-body effective mass m^* in Si inversion layers, several attempts have been made to understand these phenomena microscopically. Janak[4] first developed an elegant theory of m^* and g^* in the 2D electron gas using a static approximation to the screening. Further work in Si inversion layers along similar lines has been reported by different groups[5]. Quinn and co-workers[6,7] evaluated these quantities using the Fermi-liquid interaction approach applied previously by Rice[8] in the 3D electron gas. Vinter[9] used the plasmon-pole approximation to the dielectric function in the self-energy expression and calculated the effective mass based on a solution of an exact Dyson's equation. Rice's method was based on a much simpler on-shell approximation. Calculations including both charge- and spin-fluctuation-induced vertex corrections have been done for the inversion layer by Yarlagadda and Giuliani[10] and for the ideal 2D electron gas by Santoro and Giuliani.[11] Recently, Jang and Min[12] reported their calculations for the effective mass of the 2D electron gas using the GW approximation with several types of dielectric functions.

The purpose of the present work is to use quantum Monte Carlo methods to calculate Fermi-liquid parameters. These are directly related to the Landé g factor and the effective mass. In a previous paper,[13] we investigated ground-state properties of this system by both variational and fixed-node Green's function methods with trial wave functions including *backflow* and *three-body* correlations in addition to two-body correlation. In this paper, Landau Fermi-liquid parameters are determined by examining particle-hole excitation energies with the variational Monte Carlo (VMC) method. In the process, we find that the pair-product (Slater-Jastrow) wave function is missing an important type of correlation between particles and holes with opposite spins. Backflow correlation is crucial for calculating these interactions.

The density is parametrized by $r_s = a/a_0$, where a_0 is the Bohr radius, $a = 1/\sqrt{\pi\rho}$ is the radius of a circle which encloses one electron on the average, and ρ is the number density. Since the energy unit of Rydbergs and the length unit of a are used here, the Hamiltonian of the electron gas is

$$H = -\frac{1}{r_s^2}\sum_{i=1}\nabla_i^2 + \frac{2}{r_s}\sum_{i<j}\frac{1}{|\mathbf{r}_i - \mathbf{r}_j|} + \text{const}\,, \qquad (1)$$

where the constant is the term due to the uniform background of opposite charge. The calculations are done for the density range, $1 \le r_s \le 5$, where most of experiments

 ©1994 The American Physical Society

on this system have been done.

According to the Fermi-liquid theory,[14] the energy of a low-lying excited state in an interacting Fermi system whose distribution function differs from the ground state by δn_κ can be expressed by

$$E \simeq E_0 + \sum_\kappa \epsilon(\kappa)\,\delta n_\kappa + \frac{1}{2}\sum_{\kappa\neq\kappa'} f(\kappa,\kappa')\,\delta n_\kappa \delta n_{\kappa'}\,, \quad (2)$$

where E_0 is the ground-state energy, $\kappa = (\mathbf{k},\sigma)$ represents both momentum and spin state of a quasiparticle, $\epsilon(\kappa)$ its energy, and $\delta n_\kappa = n_\kappa - n_\kappa^0$ the difference in the occupation number of a quasiparticle κ between the ground state and an excited state. The interaction energy $f(\kappa,\kappa')$ between quasiparticles κ and κ' is of order $1/N$ since two quasiparticles are less likely to interact as the system is made larger. It can be separated into spin-symmetric and spin-antisymmetric terms:

$$f(\kappa,\kappa') \equiv f^s(\mathbf{k},\mathbf{k}') + \sigma\sigma' f^a(\mathbf{k},\mathbf{k}'), \qquad \sigma = \pm 1\,. \quad (3)$$

In a 2D isotropic Fermi liquid,[15] $f^{s(a)}(\mathbf{k},\mathbf{k}')$'s can be Fourier expanded:

$$f^{s(a)}(\mathbf{k},\mathbf{k}') = \sum_{l=0}^{\infty} f_l^{s(a)} \cos(l\theta_{\mathbf{k}\mathbf{k}'})\,, \quad (4)$$

if both $\mathbf{k}$ and $\mathbf{k}'$ lie on the Fermi surface. We work in a finite system with periodic boundary conditions. Our system is not isotropic but has the symmetry of a square. Nonisotropic effects should decrease as the system size increases and thus will be considered as "finite-size" effects and discussed later.

The usual Fermi-liquid parameters $F_l^{s(a)}$ are defined using the density of states $\nu(\epsilon_F)$ at the Fermi level ϵ_F for an infinite system:

$$F_l^{s(a)} \equiv \nu(\epsilon_F)\, f_l^{s(a)} = \frac{N r_s^2}{2}\frac{m^*}{m}\, f_l^{s(a)}\,, \quad (5)$$

where the effective mass is defined by

$$\frac{m}{m^*} \equiv \frac{r_s^2}{2\sqrt{2}}\frac{\partial\epsilon}{\partial k}\Big|_{k_F}\,. \quad (6)$$

The effective mass is also related to F_1^s by

$$\frac{m^*}{m} = 1 + \frac{1}{2}F_1^s\,. \quad (7)$$

The compressibility κ^*, the spin-susceptibility χ^*, and the Landé g factor are given by

$$\frac{\kappa}{\kappa^*} = \frac{m}{m^*}(1+F_0^s)\,, \quad \frac{\chi}{\chi^*} = \frac{m}{m^*}(1+F_0^a)\,, \quad (8)$$

and

$$g^*/g = m\chi^*/m^*\chi = (1+F_0^a)^{-1}\,, \quad (9)$$

where κ, χ, and g stand for the compressibility, the spin-susceptibility, and the Landé g factor of the noninteracting system, respectively.

There have been very few quantum Monte Carlo calculations of properties of excited states, particularly of extended systems. So we discuss the problem of calculating these Fermi-liquid parameters in some detail. Our approach is to estimate accurately the individual energies of all the lowest single particle-hole excitations. Then the excitation energies are fit by the Fermi-liquid expression to obtain estimates of the parameters. There are two important problems to be solved. First, one needs to calculate differences in energy on the order of $1/N$ of the total energy. Since these differences can easily be masked by the statistical errors, a correlated sampling approach is developed to calculate them. Second, one must determine the best way of determining the Fermi-liquid parameters from excited-state energies of finite systems of on the order of 100 electrons. To our knowledge, such calculations have not been attempted before. In what follows, we will describe the basic scheme of obtaining the Fermi-liquid parameters by the VMC method, present results, and compare them with previous analytic calculations.

II. METHODOLOGY

A. Variational Monte Carlo

In the VMC method, a random walk generated using the Metropolis algorithm[16] is used to evaluate matrix elements of a trial wave function $\Psi_T(R)$ with the correct symmetry, where a "configuration" R is a coordinate in the $2N$-dimensional space. The configurations are sampled from a probability density function, $\Psi_G^2(R)$, called the *guiding function* to emphasize its role in guiding the random walks to important regions of configuration space. The variational energy, E_T, is just the average of the local energy, $E_L(R) = H\Psi_T(R)/\Psi_T(R)$, times the weight factors $w(R) = |\Psi_T(R)|^2 \,/\, \Psi_G^2(R)$. The detailed form of our guiding function will be discussed later.

As in any other variational method, the choice of a trial wave function is very important in the VMC method to get a good upper bound to the exact energy. The usual choice for a Fermi liquid is a pair-product (Slater-Jastrow) trial function

$$\Psi_T(R) = D_\uparrow(e^{i\mathbf{k}_i\cdot\mathbf{r}_j})\, D_\downarrow(e^{i\mathbf{k}_m\cdot\mathbf{r}_n})\, \exp\left(-\sum_{i<j}^{N} u(r_{ij})\right)\,. \quad (10)$$

We use the two-body correlation function $u(r)$ that minimizes the variational ground-state energy in the random-phase approximation (RPA) as derived by Gaskell[17] and found to work well for metallic hydrogen[18] and the electron gas.[19]

In the present work, we also utilize improved trial functions which include backflow correlation whose effects on the ground-state properties were investigated in the previous paper.[13] Our improved trial wave function has the form[13,20,21]

$$\Psi_T(R) = D_\uparrow(e^{i\mathbf{k}_i\cdot\mathbf{x}_j})\, D_\downarrow(e^{i\mathbf{k}_m\cdot\mathbf{x}_n})\, \exp\left(-\sum_{i<j}^{N} u(r_{ij})\right), \tag{11}$$

where $\mathbf{x}_i$'s are "quasiparticle" coordinates displaced from the real coordinates with a backflow correlation function $\eta(r)$:

$$\mathbf{x}_i = \mathbf{r}_i + \sum_{j\neq i}^{N} \eta(r_{ij})\,(\mathbf{r}_i - \mathbf{r}_j)\,. \tag{12}$$

The state-dependent correlation, $\mathbf{k}\cdot(\mathbf{r}_i - \mathbf{r}_j)\eta(r_{ij})$, incorporates *backflow* effects originally introduced to understand the excitation spectra of liquid ^{4}He by Feynman and Cohen.[22] Unlike our previous work on the ground state of the system, we do not consider three-body correlation in this problem because it was shown to have a much smaller effect in our density range ($1 \leq r_s \leq 5$) compared to the backflow correlation.[13] A test calculation at $r_s = 5$ gave identical results for the Fermi-liquid parameters within statistical errors with or without the three-body force.

The backflow correlation function is parametrized as

$$\eta(r) = \lambda_B\, \frac{1 + s_B r}{r_B + w_B r + r^{7/2}}\,. \tag{13}$$

We determine the variational parameters in the trial wave function by minimizing the ground-state energy. The same parameters are used for all of our low-lying excited states. Further details of optimization are given in Ref. 13. Optimized values for new variational parameters in our parametrized backflow correlation function are given in Table I. These are the same as in Ref. 13 except that additional cases are presented here.

B. Particle-hole excitations

Our excited-state trial functions, either of the pair-product or backflow type, are constructed by occupying different orbitals in the Slater determinants from the ground-state trial function. The orbitals are specified by single-body momenta and spins ($\mathbf{k}$, σ). The lattice in Fig. 1 represents the momenta allowed by the periodic boundary condition and the circle shows the 2D Fermi surface for a system of $N = 58$ electrons. A set of all lattice points which are related to each other by the symmetry of a square is called a *shell*. We consider as ground states, filled shells of these lattice points. Thus our ground states are nondegenerate states of zero momentum and zero spin.

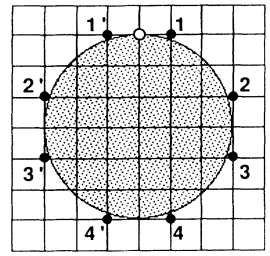

FIG. 1. Symmetrically distinctive particle-hole excitations. The lattice points correspond to single-body momenta allowed by the periodic boundary condition and the circle shows the 2D Fermi surface for a system of $N = 58$ electrons. The • and the ○ represent a particle and a hole state, respectively. All states (1–4′) shown here share the same hole. A state α' represented by a primed label is symmetrically equivalent to its corresponding unprimed state α.

We now consider all of the lowest-lying (at the Hartree-Fock level) particle-hole excitations from the ground state, where a particle is excited from a $\mathbf{k}$ point (hole state, $\mathbf{k}_h$) in the last occupied shell to a $\mathbf{k}$ point (particle state, $\mathbf{k}_p$) in the first unoccupied shell of the ground state (see Fig. 1). This excitation has the same charge and density as the ground state, thus finite-system effects should be less than would be obtained by inserting or removing an electron. According to the Fermi-liquid theory, summarized in Eq. (2), the energy of an excited state α in Fig. 1 is given by

$$E_\alpha = E_0 + \epsilon(k_p) - \epsilon(k_h) - \sum_{l=0} (f_l^s \pm f_l^a)\, \cos(l\theta_\alpha)\,, \tag{14}$$

where θ_α is the angle between $\mathbf{k}_p$ and $\mathbf{k}_h$ and the $+(-)$ sign corresponds to parallel (antiparallel) spins between particle and hole. If we know the energies of the spin-parallel and spin-antiparallel excitations considered here, we can abstract the spin-symmetric and spin-antisymmetric components, f_l^s and f_l^a, which are related to the Fermi-liquid parameters by Eq. (5).

In the example shown in Fig. 1, there are eight equivalent hole states and 16 equivalent particle states including spin degrees of freedom, thus leading to 128 excited states. But using the various symmetries of the square,

TABLE I. Optimized variational parameters of backflow correlation functions for $N = 26, 58$.

	$N = 26$				$N = 58$			
	$r_s = 1$	$r_s = 2$	$r_s = 3$	$r_s = 5$	$r_s = 1$	$r_s = 2$	$r_s = 3$	$r_s = 5$
λ_B	0.083	0.090	0.095	0.200	0.083	0.056	0.095	0.185
s_B	0.842	1.181	1.037	0.500	0.761	1.097	1.046	0.299
r_B	0.100	0.088	0.080	0.050	0.200	0.124	0.040	0.050
w_B	1.120	0.703	0.405	0.667	1.276	0.255	0.547	0.533

it is seen that there are four different spin-parallel excitations and four different spin-antiparallel excitations. Those are labeled 1–4 in Fig. 1 and hereafter. Note that each primed label shows a state symmetrically equivalent to a corresponding unprimed state.

We assume that there is no change in correlation functions (Jastrow factor and backflow) between the ground state and the excited states. Our trial function for a spin-antiparallel excitation whose particle and hole states have opposite spins is given by deleting one row of $e^{i\mathbf{k}_h\cdot\mathbf{x}_j}$ in one Slater matrix and adding one row of $e^{i\mathbf{k}_p\cdot\mathbf{x}_j}$ in the other Slater matrix. The trial wave function for a spin-parallel excitation is given by changing one row of either Slater matrix of the ground-state wave function [Eqs. (10) and (11)] from $e^{i\mathbf{k}_h\cdot\mathbf{x}_j}$ to $e^{i\mathbf{k}_p\cdot\mathbf{x}_j}$. Unlike the ground state these wave functions cannot be made real since they involve $e^{-i\mathbf{k}_h\cdot\mathbf{x}_j}$ and $e^{i\mathbf{k}_p\cdot\mathbf{x}_j}$ but not their conjugate functions $e^{i\mathbf{k}_h\cdot\mathbf{x}_j}$ and $e^{-i\mathbf{k}_p\cdot\mathbf{x}_j}$. Since we consider only single-particle excitations, the full complex wave function can be written as a sum of two real and two imaginary functions, each of which involves Slater determinants whose elements have the form $\cos(\mathbf{k}_i\cdot\mathbf{x}_j)$ or $\sin(\mathbf{k}_i\cdot\mathbf{x}_j)$. We have evaluated the matrix elements of the complex wave functions using this form. Diagonal matrix elements are purely real, which simplifies their calculation.

Even though this excited state from a spin-parallel excitation is not an eigenstate of total spin S (actually it is an eigenstate of S_z), it is a state which is appropriate for the Fermi-liquid analysis using Eq. (2) because the spin quantization axes for its all quasiparticles are the same.[23] To demonstrate that we may equally find the Fermi-liquid parameters using these spin-parallel and spin-antiparallel excitations or eigenstates of S, we have also done some test calculations using the total-spin eigenstates. We consider spin-parallel cases of an excitation α shown in Fig. 1 and call the wave function of the excitation whose particle and hole are spin up (down) $\Psi_\alpha^{(1)}$ ($\Psi_\alpha^{(2)}$). These two states are obviously degenerate. If we construct a mixed state of $\Psi_\alpha^{(m)} = \Psi_\alpha^{(1)} + e^{i\delta}\Psi_\alpha^{(2)}$, the singlet state with $S = 0$ corresponds to $\delta = 2n\pi$ and the triplet state with $S = 1$ to $\delta = (2n+1)\pi$, where n is an integer. According to the Fermi-liquid analysis in Ref. 23 applicable to the excitations whose particles and holes have different spin-quantization axes, the energy of a mixed-state $\Psi_\alpha^{(m)}$ is given by

$$E_\alpha^{(m)} = E_0 + \epsilon(k_p) - \epsilon(k_h) - f^s(\mathbf{k}_h,\mathbf{k}_p) - (2\cos\delta + 1)f^a(\mathbf{k}_h,\mathbf{k}_p)\,. \tag{15}$$

Comparing this result to Eq. (14), the mixed state with $\delta = (2n+1)\pi$ has the same energy as its corresponding spin-antiparallel excitation, which should be true because they are all degenerate triplet states with $S = 1$. In addition, the mixed state with $\delta = (n+1/2)\pi$ has the same energy as its corresponding unmixed spin-parallel excitation ($\Psi_\alpha^{(1)}$ or $\Psi_\alpha^{(2)}$). Table II shows energies of some mixed states with phase factors δ and their corresponding spin-parallel and spin-antiparallel excitations calculated for $N = 26$ at $r_s = 1$ using the VMC with the Slater-Jastrow trial functions. We have obtained the mixed-state energies by calculating both diagonal elements and off-diagonal elements between $\Psi_\alpha^{(1)}$ and $\Psi_\alpha^{(2)}$. As can be seen, the above argument from the Fermi-liquid analysis is confirmed by our VMC calculations within the statistical errors. Therefore, in order to obtain the respective Fermi-liquid parameters (F_l^s and F_l^a) from the particle-hole excitations shown in Fig. 1, we may either consider total spin eigenstates with $S = 0$ and 1 whose energies should be analyzed according to Eq. (15) or consider the spin-parallel and spin-antiparallel excitations whose energies can be analyzed according to Eq. (14). We follow the latter case in this paper because it requires only diagonal elements between $\Psi_\alpha^{(1)}$ and $\Psi_\alpha^{(2)}$ which are real.

The total momenta of these excited states, $\mathbf{k}_p - \mathbf{k}_h$, are nonzero and thus they will be orthogonal to the ground state. Thus the variational principle applies to the excited states. It is possible for two of the excited states with the same spin configuration to overlap with each other and to be degenerate. For example, the state labeled 1 in Fig. 1 and its reflected state with respect to k_x axis may have a nonzero overlap because they have the same total momentum. We could construct a state by mixing two states which has a lower energy than individual ones. However, this would require the energy expression of Eq. (2) to be reformulated in terms of matrices in the momenta, analogous to the spin case considered in Ref. 23 and discussed above. This is outside the standard framework of the Fermi-liquid theory assuming a well-defined momentum for each quasiparticle. Therefore, we neglect the overlap between the states with the same total momentum in order to apply the Fermi-liquid analysis to our calculation of particle-hole excitation energies.

In this paper, we determine various Fermi-liquid parameters using the VMC method and the Fermi-liquid expression Eq. (14). We calculate directly energy differences between several excited states, $\Delta E_{\alpha\beta} = E_\alpha - E_\beta$,

TABLE II. Energies of mixed states $\Psi_\alpha^{(m)}$ and their corresponding spin-parallel excitations and spin-antiparallel excitations using the Slater-Jastrow trial functions for $N = 26$ at $r_s = 1$. The energies are in units of Ry.

	Mixed states			spin-parallel	spin-antiparallel
	$\delta = 2n\pi$	$\delta = (2n+1)\pi$	$\delta = (n+1/2)\pi$	excitations	excitations
E_1	-8.9812(24)	-9.1651(24)	-9.0778(23)	-9.0785(23)	-9.1638(46)
E_2	-9.0322(24)	-9.1744(23)	-9.1054(23)	-9.1047(23)	-9.1757(45)
E_3	-9.0813(24)	-9.1751(24)	-9.1288(24)	-9.1286(23)	-9.1757(45)
E_4	-9.0992(23)	-9.1656(23)	-9.1326(24)	-9.1326(23)	-9.1638(46)

and determine the Fourier components f_l^s and f_l^a by fitting them to the form

$$\Delta E_{\alpha\beta} = \sum_{l=1} (f_l^s \pm f_l^a)\,[-\cos(l\theta_\alpha) + \cos(l\theta_\beta)]\,. \quad (16)$$

Then the effective mass is obtained by

$$\frac{m^*}{m} = (1 - \tfrac{1}{4} r_s^2 N f_1^s)^{-1}\,, \quad (17)$$

which follows from Eqs. (5) and (7). Other dimensionless Fermi-liquid parameters $F_l^{s(a)}$ can be determined using Eq. (5) from $f_l^{s(a)}$ and the mass.

Here we note that there is also an alternative approach for calculation of the effective mass which involves energy differences between excited states and the ground state. To simplify the calculation, only spin-parallel excitations are considered here. From Eqs. (5) and (8), we get

$$f_0^s + f_0^a = \frac{2}{N r_s^2}\left(\frac{\kappa}{\kappa^*} + \frac{\chi}{\chi^*} - 2\frac{m}{m^*}\right)\,. \quad (18)$$

And we assume that near the Fermi surface

$$\epsilon(k_p) - \epsilon(k_h) \simeq \frac{m}{m^*}\frac{1}{r_s^2}\,(k_p^2 - k_h^2)\,. \quad (19)$$

[This is better than Eq. (6) for a finite system since one does not know what to use for the Fermi wave vector in a finite system.] Inserting Eqs. (18) and (19) into Eq. (14), we get

$$\Delta E_{\alpha 0} + \frac{2}{N r_s^2}\left(\frac{\kappa}{\kappa^*} + \frac{\chi}{\chi^*}\right) = \frac{m}{m^*}\frac{1}{r_s^2}\left(k_p^2 - k_h^2 + \frac{4}{N}\right) - \sum_{l=1} (f_l^s + f_l^a)\cos(l\theta_\alpha)\,, \quad (20)$$

where $\Delta E_{\alpha 0} = E_\alpha - E_0$. If energy differences between the ground state and several excited states shown in Fig. 1 are calculated and the compressibility and spin susceptibility of the system are known, one can abstract the mass from Eq. (20). The first term is due to the one body excitation of the particle-hole pair, the second to the interaction energy of the particle-hole pair in the finite box. While the first term dominates at small r_s, they become equally important at large r_s. In Sec. III we also consider this alternative method for the effective mass using our VMC results; however, we find it less satisfactory than our other approach, because of larger finite-size effects.

C. Importance of backflow

A simple argument shows why the backflow correlation is crucial in understanding the excited-state energies. Consider two spin-antiparallel particle-hole excitations 1 and 4′ in Fig. 1 which have the same spin-up hole state and whose spin-down particle states have opposite momenta to each other. Suppose the wave function of state 1 is $\Psi_1 = D_\uparrow D_\downarrow \exp(-\phi)$ where ϕ will include ground-state (bosonic) correlations. The wave function of state 4′ is $\Psi_{4'} = D_\uparrow D_\downarrow^* \exp(-\phi)$, where D^* indicates a complex conjugate. The probability densities, i.e., the squared modulus, of two wave functions are obviously the same. Explicit calculation shows that the real part of the local-energy difference between two states is given by

$$\mathrm{Re}[E_L(1) - E_L(4')] = -\frac{2}{r_s}\sum_i \mathrm{Re}\left[\frac{\nabla_i D_\uparrow}{D_\uparrow}\cdot\left(\frac{\nabla_i D_\downarrow}{D_\downarrow} - \frac{\nabla_i D_\downarrow^*}{D_\downarrow^*}\right)\right]\,. \quad (21)$$

(Of course the average imaginary part of the local energy vanishes.) If the wave functions are of the Slater-Jastrow type, this real part of the local-energy difference is zero since it is a sum of terms $\nabla_i D_\uparrow \cdot \nabla_i D_\downarrow$, where the derivatives of the determinants are taken with respect to only one electron i. Clearly each term vanishes since a given electron belongs to only one of the determinants. Therefore, two states 1 and 4′ have the same variational energy. It follows that all odd order spin-antisymmetric Fermi liquid parameters are equal to their corresponding spin-symmetric parameters [see Eq. (16)]. This is a defect of the Slater-Jastrow wave function and is the reason why the backflow correlation is so important to account for particle-hole excitations. On the other hand, the quasiparticle coordinate $\mathbf{x}_i$ is affected by the positions of all particles through backflow correlation [see Eqs. (11) and (12)] so that backflow trial functions do not have this defect in general. Our results show that energies in this pair of states is highly correlated, so the difference can be more easily computed.

D. Correlated sampling method

Energy differences between the excited states under consideration are very small because they are determined by the second-order terms in the total energy expression of Eq. (2). In order to calculate very small energy differences, we use a correlated sampling method, where energies of all related states are calculated with the same set of configurations.

We sample configurations from a *guiding function* Ψ_G and then use the set of configurations to determine all of the relevant state energies as ratios of weighted sums. The energy of state α is given by

$$E_\alpha = \frac{\sum_i w_\alpha(R_i)\, E_L^\alpha(R_i)}{\sum_i w_\alpha(R_i)}\,, \quad (22)$$

where R_i's are a series of random walkers in $2N$ dimension sampled with the probability density proportional to Ψ_G^2, $E_L^\alpha = H\Psi_\alpha/\Psi_\alpha$ is a local energy of state α, and $w_\alpha(R_i) = |\Psi_\alpha(R_i)|^2/\Psi_G^2(R_i)$ is the weight in state α. The local energies between the various states are highly correlated since all the potential energy terms are the same and the kinetic energy coming from the pair correlation is the same. Thus in taking energy difference between states, much of the noise is canceled out.

The optimization of the guiding function has been considered in Ref. 26. Clearly it must be chosen to be nonzero at any point in configuration space where any of the states under consideration are nonzero. We use the form

$$\Psi_G^2(R) = a_0 \Psi_0^2(R) + \sum_\alpha |\Psi_\alpha(R)|^2 , \qquad (23)$$

where Ψ_0 is the trial function for the ground state, Ψ_α for excited state α, and a_0 is a constant. The sum in Eq. (23) is over all excited states to be calculated. In order to calculate energy differences between the ground state and excited states, a_0 should not be zero. After some numerical experimentation, for the spin-parallel excitations, we found that a_0 should be approximately set to the number of excitations considered. As seen below, this choice of parameter a_0 makes the correlated sampling quite efficient between the excited states as well as between the ground state and the excited states.

There is a computational difficulty in calculating energy differences between the ground state and excited states in the spin-antiparallel excitations with correlated sampling because two Slater determinants in the excited states have different sizes from corresponding ones in the ground state. For a given configuration, we need to calculate Slater determinants and their first and second derivatives in all states involved. If the Slater matrices have the same size and we know the cofactor matrix of one Slater matrix (for example, of the ground state), then we can quickly calculate all Slater determinants and their derivatives of the other states. This is more complicated for different-sized matrices. We do not consider this difficulty here because all Fermi-liquid parameters can be calculated from Eq. (16) using only cases with same-sized matrices. Furthermore, even if one uses Eq. (20) which involves the energy differences between the ground state and excited states, one can nevertheless find the effective mass using only spin-parallel excitations. Hence we do one calculation to find the energy differences between the spin-parallel excitations (and the ground state) and another calculation with $a_0 = 0$ to find the energy differences between the spin-antiparallel excited states.

Table III shows energies of the ground state and four different spin-parallel excitations along with energy differences between them calculated for $N = 58$ at $r_s = 1$ by the correlated sampling method. Diagonal elements show the energy of each state, and off-diagonal elements show the energy differences. With the Slater-Jastrow functions, the energy difference ΔE_{14} between states 1 and 4 has error of 4.6×10^{-3} while E_1 and E_4 have error of 1.7×10^{-2}. The error bar of the energy difference must be calculated directly since the energy estimators in the various states are highly correlated. The error in a Monte Carlo calculation is inversely proportional to the square root of computer time. Hence the correlated method is about 54 times as efficient as the ordinary method where E_1 and E_4 are calculated with independent runs. One gains in efficiency both because the energies are correlated and because the calculation of the local energies of many excited states at once is much faster than doing the calculations separately. For example, w_α in Eq. (22) is obtained from a dot product of one row of the cofactor matrix of the ground-state Slater determinant with the corresponding row of the excited-state Slater determinant which involves the particle-state orbitals. This only takes N operations, as opposed to doing a new random walk which takes N^3 operations. The local energies for the excited states can be obtained from the ground-state local energy and cofactor matrices with the order of N^2 operations/state for the Slater-Jastrow wave functions. Using the backflow wave functions, we have about the same gain in efficiency. We also note that the statistical error of the energy difference depends upon the states involved. It is much smaller for the cases when the particles of two states have opposite momentum while sharing the same hole state [for example, 1 and 4′(or 4) in Fig. 1]. This point will be mentioned again in the next section.

We have also checked how the correlated sampling

TABLE III. Energies (E_α) of and energy differences ($\Delta E_{\alpha\beta} = E_\alpha - E_\beta$) between particle-hole excitations whose particle state and hole state have parallel spins. Results for the states with the same symmetry have been combined together. Calculations are done for $N = 58$ at $r_s = 1.0$ (S.J.: Slater-Jastrow wave function, B.F.: backflow wave function). State 0 means the ground state and states 1–4 are excitations as labeled in Fig. 1. A diagonal element represents energy of each state and an off-diagonal element shows energy difference between the state in the row and one in the column. About 10^5 configurations were averaged over for the Slater-Jastrow energies, about 4×10^5 for the backflow energies. The energies are in units of Ry.

		E_0	E_1	E_2	E_3	E_4
	E_0	-22.5150(190)	-0.2570(110)	-0.2370(120)	-0.2270(120)	-0.2280(110)
	E_1		-22.2580(170)	0.0203(62)	0.0299(63)	0.0291(46)
S.J.	E_2			-22.2780(170)	0.0096(40)	0.0085(65)
	E_3				-22.2880(180)	-0.0008(69)
	E_4					-22.2870(170)
	E_0	-23.3280(70)	-0.2360(100)	-0.2190(100)	-0.2160(100)	-0.2080(110)
	E_1		-23.0920(120)	0.0170(30)	0.0205(30)	0.0285(36)
B.F.	E_2			-23.1090(130)	0.0035(19)	0.0115(37)
	E_3				-23.1130(130)	0.0081(35)
	E_4					-23.1210(140)

method scales with the number of particles. Since physical quantities which should be size independent are expressed in terms of Nf_l's, we compare here CPU times which give the same statistical error in $N(f_1^s + f_1^a)$ in different size calculations at $r_s = 5$. Using the Slater-Jastrow trial function, we find the CPU time needed for equally accurate results scales as the fourth power of the number of particles between $N = 28$ and 98 This is exactly the scaling one expects from an uncorrelated method of calculating energy differences. Thus our method has only changed the prefactor of the scaling of the CPU time with N (by roughly a factor of 100), not the exponent. With the backflow wave functions, the exponent goes as roughly 5 between $N = 26$ and 58. This is because of the increased computational work as explained in Ref. 13. As expected, increase in the system size is more expensive with the backflow wave function than with the Slater-Jastrow wave function. The calculations reported here take on the order of 10^3 hours on an IBM RS6000 workstation. It is likely that these correlated sampling methods would be much more efficient in systems where the electrons are localized, i.e., in an insulator. There the excited state would only differ from the ground state in a localized region, not throughout the whole simulation cell.

One might worry that because the backflow functions have only been optimized in the ground state the excited-state energies will be systematically higher. With variational methods, one always must be concerned about such a bias. But we notice from Table III that actually the excited states drop about 2.2% more than the ground state so that backflow correlations are more important in the excited states, possibly because they have nonzero momenta. We hope that relative energy differences between the excited states will be less affected by a bias. We intend to check if such a bias exists by a Green's function Monte Carlo calculation of excited-state energies. We see that state 1 gains most energy by including backflow correlation. That is related to the mass increase with backflow, which will be reported in the next section.

III. EFFECTIVE MASS AND OTHER FERMI-LIQUID PARAMETERS

In this section we present results for Fermi-liquid parameters obtained by analyzing quantum Monte Carlo calculations of the particle-hole excitation energies according to Eq. (14). Our results for the effective mass will be compared to the ones previously obtained by several analytic methods.

We consider separately two kinds of excitations, one whose particle state and hole state have parallel spins and one with antiparallel spins to find the respective spin-symmetric and spin-antisymmetric Fermi-liquid parameters. In order to extrapolate our results to the thermodynamic limit, the finite-size effects must be removed. We anticipate that the effect of small system sizes that we use will be canceled out in energy differences between excited states. We first try to confirm this by examining the effective mass using Slater-Jastrow wave functions for which we can more easily study their size dependence.

A. Slater-Jastrow calculations

As discussed above, there are two ways to use our results to find the effective mass. In order to calculate the mass from energy differences between the ground state and excited states [Eq. (20)], we need to know the compressibility and the spin susceptibility of the system. The compressibility of the electron gas can be calculated using

$$\frac{\kappa}{\kappa^*} = 1 - \frac{\sqrt{2}r_s}{\pi} + \frac{r_s^4}{8}\left(\frac{d^2}{dr_s^2} - \frac{1}{r_s}\frac{d}{dr_s}\right)E_c(r_s)\,, \qquad (24)$$

where $E_c(r_s)$ is the correlation energy per electron. We obtain the compressibility from the correlation energy calculated in our previous work.[13] The spin susceptibility was estimated by calculating the energies to flip entire shells of spins by Tanatar and Ceperley.[24] By fitting the energy differences to Eq. (20), we obtain the many-body effective mass of the system. The mass with this method shows very strong size dependence. At $r_s = 5.0$, m^*/m is 1.61(3) for $N = 26$, 2.07(13) for $N = 58$, and 1.51(7) for $N = 98$. We do not understand quantitatively why the effective mass calculated this way is sensitive to the size of the system and gives different results from our other method which we are about to discuss. We have not pursued this point because it seems likely that the system size affects differently the ground state and the low-lying excited states. Another possibility is that there is a systematic effect coming from using wave functions optimized only in the ground state.

We now investigate the mass calculated by our method which uses only energy differences between excited states [Eqs. (16) and (17)]. Since the effective mass is related to F_1^s which is equal to F_1^a with the Slater-Jastrow wave function, we need consider only spin-parallel excitations. Recall that Nf_l should be independent of system size because the interaction term f between quasiparticles is of order N^{-1}. We do a least-squares fit of $N\Delta E_{\alpha\beta}$ using Eq. (16) to determine the best parameters Nf_l, where $1 \le l \le 3$ with all of the excited states. These are shown in Table IV for $N = 26, 58, 98$ at $r_s = 5.0$. As can be seen, our results for Nf_l's are independent of the system size within the statistical errors. The bottom row of Table IV shows the results by one fit of considering the whole data from three different sizes at once. The reasonable χ^2 value shows that the results are independent of N within our statistical errors. The effective mass determined from Eq. (17) is found to be about $0.9m$ with very

TABLE IV. Spin-parallel Fourier components $f_l^s + f_l^a$ at $r_s = 5.0$ obtained by fitting energy differences between the excited states to Eq. (16). The calculations are done with the Slater-Jastrow wave functions. The bottom row represents ones by fitting all calculations of different sizes at once. The unit of the components is Ry.

	$N(f_1^s + f_1^a)$	$N(f_2^s + f_2^a)$	$N(f_3^s + f_3^a)$	χ^2
$N = 26$	-0.034(1)	-0.001(1)	-0.001(1)	
$N = 58$	-0.036(6)	-0.000(7)	-0.001(6)	
$N = 98$	-0.038(8)	-0.001(7)	-0.001(8)	
	-0.034(1)	-0.001(1)	-0.001(1)	0.34

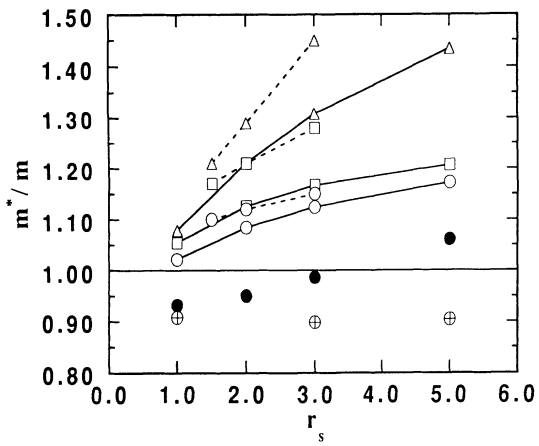

FIG. 2. The effective mass vs the density parameter r_s in the 2D electron gas. Our Monte Carlo estimation with the Slater-Jastrow and the backflow wave functions is shown by $\oplus$ and $\bullet$, respectively. The dotted lines show the results calculated by Lee *et al.* (Ref. 7) with different schemes ($\triangle$: Rice's method; $\bigcirc$: Vinter's method; and $\square$: Hedin and Lundquist's method). The solid lines show the results using the *GW* approximation with various dielectric functions in Ref. 12 ($\bigcirc$: RPA; $\triangle$: Hubbard approximation; and $\square$: modified Hubbard approximation).

little density dependence throughout our density range ($1 \leq r_s \leq 5$) (see Fig. 2 and Table V).

Finally, we note that there is yet a third way to estimate the effective mass. In analyzing the finite-size effects in the Slater-Jastrow calculations for the ground state, Tanatar and Ceperley[24] argued that one of their fitted parameters, $b_1(r_s)$, corresponds to the inverse of the effective mass. In order to extrapolate to the thermodynamic limit, they used the following scaling equation:

$$E_N = E_\infty + b_1(r_s)\,\Delta T_N + b_2(r_s)\,\frac{1}{N}\,, \tag{25}$$

where E_N and E_∞ is the energies of a finite system with periodic boundary condition and the infinite system, respectively, and ΔT_N is the difference between the kinetic energies of N noninteracting electrons and the infinite system at $r_s = 1$. Considering Eq. (2) but now taking for δn_κ the difference in occupation of a finite system and the infinite system, the energy of a finite system can be expressed by

$$E_N = E_\infty + \frac{m}{m^*}\frac{\Delta T_N}{r_s^2} + \cdots \tag{26}$$

within the parabolic assumption, Eq. (19), of the quasiparticle energy spectra. By comparing Eq. (26) with (25), we see that $r_s^2 b_1(r_s)$ corresponds to m/m^*. Their result for the mass is $m^*/m = 0.90(1), 0.97(5)$ for $r_s = 1, 5$. We also obtained the same parameter in our ground-state work,[13] which leads to $m^*/m = 0.90(1), 0.90(5)$ for $r_s = 1, 5$. These values from the ground-state calculations are quite consistent with our present results derived from energy differences between the excited states. All results for the effective mass calculated with the Slater-Jastrow trial functions are summarized in Table V.

We have seen so far from the Slater-Jastrow calculations that the method for computing the effective mass from energy differences between the excited states gives results that have small dependence on the system size. In fact, as is shown in Table V (part II), all results from this method are independent of the system size to within the statistical errors. Since we are unable to carry out backflow calculations on the largest system we consider only the two smaller sizes for the backflow excited-state calculations.

B. Backflow calculations

To get improved estimations for the effective mass and other Fermi-liquid parameters, we now use the backflow wave functions. Only energy differences between excited states are considered here because, as we have discussed in the previous section, this method leads to results which are little affected by the system size and are consistent with ones derived from the ground-state calculations. These calculations are done for $N = 26, 58$ at $r_s = 1, 2, 3, 5$, with the results for the cases of spin-parallel excitations and spin-antiparallel excitations shown in Tables VI and VII, respectively. The energy differences between some states have much smaller statistical uncertainty than others, especially for spin-antiparallel excitations, because some states are more correlated with each other. In fact, the states having the most statistical correlation are degenerate at the Slater-Jastrow level. They are the ones that we discussed in Sec. II C. Apparently the statistical fluctuations in these states are almost identical since the differences only come from the backflow terms. As can be seen, all fits have reasonable χ^2 values.

Combining fitted values for the first-order components, $f_l^s \pm f_l^a$, in Tables VI and VII, we determine the effective mass of the system from Eq. (17). The results for m^* are given in Table VIII along with the dimensionless Fermi-liquid parameters F_l^s and F_l^a defined in Eq. (5). Figures

TABLE V. The effective mass obtained by several different methods with the Slater-Jastrow wave functions. I corresponds to the method where the energy differences between the ground state and excited states are analyzed and II to the method where the energy differences between excited states are analyzed. III shows the masses obtained from finite-size analysis of ground-state calculations [*a*: Tanatar and Ceperley's work (Ref. 24). *b*: Our ground-state work (Ref. 13)].

		$r_s = 1.0$	$r_s = 3.0$	$r_s = 5.0$
I	N=26	1.07(1)	1.21(2)	1.61(3)
	N=58	1.02(2)	1.23(3)	2.07(13)
	N=98	1.24(5)		1.51(7)
II	N=26	0.91(1)	0.90(1)	0.90(1)
	N=58	0.90(1)	0.89(1)	0.90(3)
	N=98	0.90(2)		0.89(3)
III	*a*	0.90(1)		0.97(5)
	b	0.90(1)		0.91(5)

TABLE VI. Energy differences ($\Delta E_{\alpha\beta} = E_\alpha - E_\beta$) between particle-hole excitations whose particle state and hole state have parallel spins. States 1–4 are excitations shown in Fig. 1. Calculations are done with the backflow wave functions. Values for parameters fitted to Eq. (16) are shown at the bottom along with χ^2 values. Energy unit is Ry.

		$r_s = 1$	$r_s = 2$	$r_s = 3$	$r_s = 5$
	$N\Delta E_{12}$	0.5(1)	0.16(4)	0.07(2)	0.029(9)
	$N\Delta E_{13}$	1.0(2)	0.30(4)	0.12(2)	0.033(8)
	$N\Delta E_{14}$	1.2(2)	0.32(2)	0.11(1)	0.020(5)
$N = 26$	$N\Delta E_{23}$	0.5(2)	0.14(3)	0.05(1)	0.004(6)
	$N\Delta E_{24}$	0.7(2)	0.16(4)	0.05(2)	-0.008(8)
	$N\Delta E_{34}$	0.2(2)	0.03(3)	-0.01(2)	-0.011(8)
	$N\Delta E_{12}$	1.0(2)	0.18(8)	0.13(4)	0.011(20)
	$N\Delta E_{13}$	1.2(2)	0.31(7)	0.17(4)	0.024(20)
	$N\Delta E_{14}$	1.6(3)	0.38(4)	0.16(2)	0.027(14)
$N = 58$	$N\Delta E_{23}$	0.2(2)	0.12(3)	0.04(3)	0.012(13)
	$N\Delta E_{24}$	0.7(3)	0.19(8)	0.03(4)	0.016(21)
	$N\Delta E_{34}$	0.5(3)	0.07(7)	-0.00(4)	0.003(20)
	$N(f_1^s + f_1^a)$	-0.69(5)	-0.18(1)	-0.064(3)	-0.011(2)
	$N(f_2^s + f_2^a)$	-0.13(5)	-0.05(2)	-0.031(5)	-0.014(3)
	$N(f_3^s + f_3^a)$	-0.11(4)	-0.01(1)	-0.003(3)	-0.002(2)
	χ^2	4.0	2.1	5.4	4.8

2 and 3 show the mass as a function of the density calculated by our VMC method along with some previously-calculated values using various other methods. We see significant mass enhancement from the Slater-Jastrow values by including backflow correlations over the density range considered. Our effective mass has quite different values from ones calculated by other methods. Note that the mass m^*/m is less than 1 for $r_s < 3$ and increases to > 1 for larger r_s. It has rather similar density dependence to one calculated for the 3D electron gas by Rice.[8] According to Fig. 3, our mass turns out to be close to that obtained by Santoro and Giuliani[11] when including only charge-fluctuation-induced vertex corrections beyond RPA. However, our results do not agree with their results that include both charge and spin fluctuations. The spin fluctuations were claimed to be important to give correct "bandwidth" masses $\bar{m}$, which are defined by $\hbar^2 k_F^2/2\bar{m} = \epsilon(k_F) - \epsilon(0)$, in "jellium" metals such as Na, Al, etc. by Zhu and Overhauser.[25]

From the previous Monte Carlo results for the compressibility from Ref. 13 and the spin susceptibility by Tanatar and Ceperley[24] along with the effective mass determined here, we can obtain the zeroth-order parameters, F_0^s and F_0^a, through Eq. (8). Note that the Landé

TABLE VII. Energy differences ($\Delta E_{\alpha\beta} = E_\alpha - E_\beta$) between particle-hole excitations whose particle state and hole state have antiparallel spins. States 1–4 are excitations shown in Fig. 1. Calculations are done with the backflow wave functions. Values for parameters fitted to Eq. (16) are shown at the bottom along with χ^2 values. Energy unit is Ry.

		$r_s = 1$	$r_s = 2$	$r_s = 3$	$r_s = 5$
	$N\Delta E_{12}$	0.20(14)	0.09(6)	0.088(19)	0.074(11)
	$N\Delta E_{13}$	0.09(13)	0.03(6)	0.033(19)	0.040(11)
	$N\Delta E_{14}$	-0.20(1)	-0.14(1)	-0.095(3)	-0.053(2)
$N = 26$	$N\Delta E_{23}$	-0.10(2)	-0.07(1)	-0.053(3)	-0.035(2)
	$N\Delta E_{24}$	-0.39(12)	-0.23(6)	-0.184(19)	-0.127(11)
	$N\Delta E_{34}$	-0.29(13)	-0.17(5)	-0.129(19)	-0.092(10)
	$N\Delta E_{12}$	0.13(14)	0.18(8)	0.133(41)	0.051(23)
	$N\Delta E_{13}$	0.06(14)	0.14(8)	0.096(42)	0.030(23)
	$N\Delta E_{14}$	-0.19(2)	-0.12(1)	-0.085(5)	-0.048(3)
$N = 58$	$N\Delta E_{23}$	-0.08(2)	-0.04(1)	-0.037(5)	-0.022(3)
	$N\Delta E_{24}$	-0.33(14)	-0.29(8)	-0.218(41)	-0.099(24)
	$N\Delta E_{34}$	-0.24(14)	-0.26(8)	-0.180(41)	-0.079(23)
	$N(f_1^s - f_1^a)$	0.108(4)	0.074(3)	0.052(2)	0.029(1)
	$N(f_2^s - f_2^a)$	-0.15(4)	-0.12(2)	-0.092(7)	-0.061(4)
	$N(f_3^s - f_3^a)$	-0.001(1)	-0.001(3)	-0.004(2)	-0.004(1)
	χ^2	3.1	7.5	5.3	14.8

TABLE VIII. Fermi-liquid parameters, the effective mass, and the Landé g factor calculated variationally with backflow wave functions. The zeroth-order parameters are obtained from the compressibility from Ref. 13 and the spin-susceptibility data in Ref. 24 along with our effective mass.

	$r_s = 1.0$	$r_s = 2.0$	$r_s = 3.0$	$r_s = 5.0$
F_0^s	-0.60(1)	-0.99(1)	-1.63(1)	-3.70(3)
F_0^a	-0.34(3)	-0.41(8)	-0.49(7)	-0.5(1)
F_1^s	-0.14(2)	-0.10(1)	-0.03(1)	0.12(2)
F_1^a	-0.19(2)	-0.24(1)	-0.26(1)	-0.27(2)
F_2^s	-0.07(2)	-0.16(3)	-0.27(3)	-0.50(5)
F_2^a	0.01(2)	0.07(3)	0.14(3)	0.32(5)
m^*/m	0.93(1)	0.95(1)	0.99(1)	1.06(1)
g^*/g	1.52(6)	1.7(2)	2.0(3)	1.9(4)

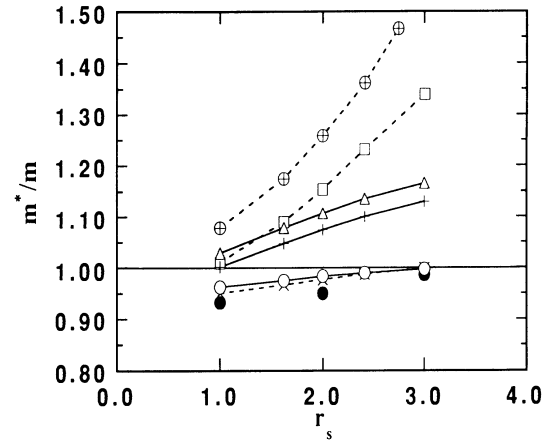

FIG. 3. The effective mass vs the density parameter r_s in the 2D electron gas. Our Monte Carlo estimation with the backflow wave functions is shown by •. The dotted lines show the results including charge- and spin-fluctuation-induced vertex corrections with an on-shell approximation (⊕ : RPA; × : charge fluctuation only; and □ : charge and spin fluctuation) and the solid lines show the results with an exact Dyson's equation (△ : RPA; ○ : charge fluctuation only; and + : charge and spin fluctuation) in Ref. 11.

g factor is determined by only F_0^a. Table VIII shows the Fermi-liquid parameters, the effective mass, and the Landé g factor obtained by our best variational calculation.

IV. CONCLUSION

We have investigated particle-hole excitations in the 2D electron gas with the VMC method. We have found from a simple argument that the pair-product (Slater-Jastrow) wave functions have a serious defect and backflow correlations are crucial. We use the form of backflow which was previously shown to significantly improve the ground-state energies[13] and here we find a significant mass increase with the backflow correlation.

We have developed a correlated sampling method which is very efficient for calculation of small energy differences between excitations which are closely related. Fermi-liquid parameters are determined from these energy differences. We have tested various approaches to the derivation of the Fermi-liquid parameters, especially the effective mass, from our VMC calculation of particle-hole excitation energies, and we have shown that the problems introduced by finite-size effects are best eliminated if we use a method involving only energy differences between the excited states with the same number of electrons.

Our primary results are given in Table VIII and compared with previous work in Figs. 2 and 3. Our effective mass is less than bare electron mass m for $r_s < 3$ and greater than m for larger r_s. This density dependence is similar to Rice's results[8] for the 3D electron gas. Our results for the effective mass are close to ones calculated including only charge-fluctuation-induced vertex corrections by Santoro and Giuliani; however, they are significantly different from other previous results. Using our calculated mass along with the previous Monte Carlo calculations of the compressibility and the spin susceptibility, we have estimated the zeroth-order Fermi-liquid parameters, F_0^s and F_0^a.

We emphasize that the present results are variational and depend upon the accuracy of our variational function. In order to go beyond this variational study, transient estimate calculations of the excited-state energy differences with the method proposed by Ceperley and Bernu[26] are in progress.

ACKNOWLEDGMENTS

We would like to thank G. Ortiz, G. Engel, and V. Rao for helpful discussions. This work has been supported by the Department of Energy under Contract No. DEFG 02-91-ER45439 and the National Science Foundation under Grant No. NSF DMR 91-17822. The calculations were performed on the CRAY YMP at the National Center for Supercomputing Applications and IBM RISC/6000 workstations in the Materials Research Laboratory at the University of Illinois.

[1] T. Ando, A. Fowler, and F. Stern, Rev. Mod. Phys. **54**, 437 (1982).
[2] F. F. Fang and P. J. Stiles, Phys. Rev. **174**, 823 (1968).
[3] J. L. Smith and P. J. Stiles, Phys. Rev. Lett. **29**, 102 (1972).
[4] J. F. Janak, Phys. Rev. **178**, 1416 (1969).
[5] K. Suzuki and Y. Kawamoto, J. Phys. Soc. Jpn. **35**, 1456 (1973); T. Ando and Y. Uemura, *ibid.* **37**, 1044 (1974).
[6] C. S. Ting, T. K. Lee, and J. J. Quinn, Phys. Rev. Lett. **34**, 870 (1975); T. K. Lee, C. S. Ting, and J. J. Quinn, *ibid.* **35**, 1048 (1975).
[7] T. K. Lee, C. S. Ting, and J. J. Quinn, Surf. Sci. **58**, 246 (1976).

[8] T. M. Rice, Ann. Phys. **31**, 100 (1965).
[9] B. Vinter, Phys. Rev. Lett. **35**, 1044 (1975); Phys. Rev. B **13**, 4447 (1976).
[10] S. Yarlagadda and G. F. Giuliani, Phys. Rev. B **38**, 10 966 (1988); Surf. Sci. **229**, 410 (1990).
[11] G. E. Santoro and G. F. Giuliani, Solid State Commun. **67**, 681 (1988); Phys. Rev. B **39**, 12 818 (1989).
[12] Y. -R. Jang and B. I. Min, Phys. Rev. B **48**, 1914 (1993).
[13] Y. Kwon, D. M. Ceperley, and R. M. Martin, Phys. Rev. B **48**, 12 037 (1993).
[14] D. Pines and P. Nozières, *The Theory of Quantum Liquids* (Addison-Wesley, Reading, MA, 1989), Vol. 1.
[15] R. Freedman, Phys. Rev. B **18**, 2482 (1978).
[16] N. Metropolis, A. Rosenbluth, M. Rosenbluth, A. H. Teller, and E. Teller, J. Chem. Phys. **21**, 1087 (1953).
[17] T. Gaskell, Proc. Phys. Soc. London **77**, 1182 (1961).
[18] D. M. Ceperley and B. J. Alder, Phys. Rev. B **36**, 2092 (1987).
[19] D. Ceperley, Phys. Rev. B **18**, 3126 (1978).
[20] K. E. Schmidt, M. A. Lee, and M. H. Kalos, Phys. Rev. Lett. **47**, 807 (1981).
[21] R. M. Panoff and J. Carlson, Phys. Rev. Lett. **62**, 1130 (1989).
[22] R. P. Feynman and M. Cohen, Phys. Rev. **102**, 1189 (1956).
[23] G. Baym and C. Pethick, *Landau Fermi Liquid Theory* (Wiley, New York, 1991).
[24] B. Tanatar and D. M. Ceperley, Phys. Rev. B **39**, 5005 (1989).
[25] X. Zhu and A. W. Overhauser, Phys. Rev. B **33**, 925 (1986).
[26] D. M. Ceperley and B. Bernu, J. Chem. Phys. **89**, 6316 (1988); B. Bernu, D. M. Ceperley, and W. A. Lester, Jr., *ibid.* **93**, 552 (1990).

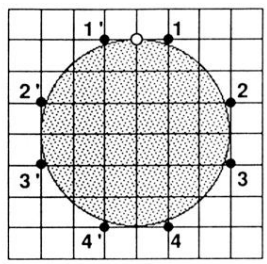

FIG. 1. Symmetrically distinctive particle-hole excitations. The lattice points correspond to single-body momenta allowed by the periodic boundary condition and the circle shows the 2D Fermi surface for a system of $N = 58$ electrons. The $\bullet$ and the $\bigcirc$ represent a particle and a hole state, respectively. All states (1–4′) shown here share the same hole. A state α' represented by a primed label is symmetrically equivalent to its corresponding unprimed state α.